Incoherent production of charmonia off nuclei as a good tool for the study of color transparency

J. Nemchik
Institute of Experimental Physics, Slovak Academy of Sciences, Watsonova 47, 04353 Kosice, Slovakia
(Received 17 June 2002; published 17 October 2002)

Within a light-cone QCD formalism incorporating color transparency, coherence length effects, and gluon shadowing, we study electroproduction of J/Ψ off nuclei. In contrast to light vector meson production when at small and medium energies color transparency and coherence length effects are not easily separated, in charmonium production color transparency effects dominate. We found rather large color transparency effects in the range of $Q^2 \leqslant 20$ GeV^2. They are stronger at low than at high energies and can be easily identified by the planned future experiments. Model calculations explain well the data of the New Muon Collaboration on the Sn/C ratio of nuclear transparencies as a function of the photon energy. We provide predictions for incoherent and coherent charmonium production for future measurements.

DOI: 10.1103/PhysRevC.66.045204 PACS number(s): 13.60.Le, 25.30.Rw, 25.20.Lj

I. INTRODUCTION: SPACE-TIME PATTERN OF CHARMONIUM PRODUCTION

The dynamics of charmonium production has been a hot topic evolved intensively during almost the last three decades. Discovery of J/Ψ in 1973 confirmed the idea of charm quark and gave a basis for its further investigations, affected also by further experiments carried out at new accelerators using more powerful electronics. Later, at the beginning of 1990's the experiments with relativistic heavy-ion collisions [1] stimulated the enhanced interest about charmonium suppression as a possible indication of the quark-gluon plasma formation. This fact became a motive power in investigation of space-time pattern of charmonium production and opened new possibilities to analyze various consequent phenomena.

One of the fundamental phenomena coming from QCD is color transparency (CT), studied intensively for almost the last two decades. This phenomenon can be treated either in the hadronic or in the quark basis. The former approach leads to Gribov's inelastic corrections [2], the latter one manifests itself as a result of color screening [3,4]. Although these two approaches are complementary, the quark-gluon interpretation is more intuitive and straightforward. Colorless hadrons can interact only because color is distributed inside them. If the hadron transverse size r tends to zero then the interaction cross section $\sigma(r)$ vanishes as r^2 [3]. As a result, the nuclear medium is more transparent for smaller transverse size of the hadron. Besides, this fact naturally explains the correlation between the cross sections of hadrons and their sizes [5–7].

Investigation of diffractive electroproduction of vector mesons off nuclei is very effective and sensitive for the study of CT. A photon of high virtuality Q^2 is expected to produce a pair with a small $\sim 1/Q^2$ transverse separation.[1] Then CT manifests itself as a vanishing absorption of the small sized colorless $\bar{q}q$ wave packet during propagation through the nucleus. Dynamical evolution of the small sized $\bar{q}q$ pair to a normal sized vector meson is controlled by the time scale, called formation time. Due to the uncertainty principle, one needs a time interval to resolve different levels V (the ground state) or V' (the next excited state) in the final state. In the rest frame of the nucleus this formation time is Lorentz dilated,

$$t_f = \frac{2\nu}{m_{V'}^2 - m_V^2}, \tag{1}$$

where ν is the photon energy. A rigorous quantum-mechanical description of the pair evolution was suggested in Ref. [8] and is based on the light-cone Green function technique. A complementary description of the same process in the hadronic basis is presented in Ref. [9].

Another phenomenon known to cause nuclear suppression is the effect of quantum coherence. It results from destructive interference of the amplitudes for which the interaction takes place on different bound nucleons. It reflects the distance from the absorption point when the pointlike photon becomes the hadronlike $\bar{q}q$ pair. This may also be interpreted as a lifetime of $\bar{q}q$ fluctuation providing the time scale which controls the shadowing. Again, it can be estimated by relying on the uncertainty principle and Lorentz time dilation as

$$t_c = \frac{2\nu}{Q^2 + m_V^2}. \tag{2}$$

It is usually called coherence time, but we will also use the term coherence length (CL), since light-cone kinematics is assumed, $l_c = t_c$ (similarly, for formation length $l_f = t_f$). CL is related to the longitudinal momentum transfer $q_c = 1/l_c$ in $\gamma^* N \to VN$, which controls the interference of the production amplitudes from different nucleons.

Exclusive production of vector mesons at high energies is controlled by the small-x_{Bj} (x_{Bj} is the Bjorken variable) physics, and gluon shadowing becomes an important phe-

[1]For production of light vector mesons (ρ^0, Φ^0) very asymmetric pairs can be possible when either q or $\bar{q}$ carries almost the whole photon momentum. As a result, the $\bar{q}q$ pair can have a large separation, see Sec. II and Eq. (17). However, it is not so for the production of charmonia, where mainly symmetric $\bar{q}q$ pairs (either q or $\bar{q}$ carries one half of the whole photon momentum) dominate.

nomenon [10]. It was shown in Ref. [11] that for electroproduction of charmonia off nuclei the gluon shadowing starts to be important at center-of-mass system (c.m.s.) energies $\sqrt{s} \geqslant 30$–60 GeV, depending on nuclear target and Q^2. Although the gluon shadowing is quite small in the kinematic range important for investigation of CT and discussed in the present paper, we include it in all calculations.

In electroproduction of vector mesons off nuclei one needs to disentangle CT (absorption) and CL (shadowing) as the two sources of nuclear suppression. Detailed analysis of the CT and CL effects in electroproduction of vector mesons off nuclei showed [10] that one can easily identify the difference of the nuclear suppression corresponding to absorption and shadowing in two limiting cases which can be illustrated for the example of vector dominance model (VDM).

(i) In the limit of small l_c, shorter than the mean internucleon spacing ~ 2 fm, only final state absorption matters. The ratio of the quasielastic (or incoherent) $\gamma^* A \to VX$ and $\gamma^* N \to VX$ cross sections, usually called nuclear transparency (Tr), reads [8]

$$\begin{aligned} \mathrm{Tr}_A^{inc}|_{l_c \ll R_A} &\equiv \frac{\sigma_V^{\gamma^* A}}{A \sigma_V^{\gamma^* N}} = \frac{1}{A} \int d^2b \int_{-\infty}^{\infty} dz\, \rho_A(b,z) \\ &\quad \times \exp\left[-\sigma_{in}^{VN} \int_z^{\infty} dz' \rho_A(b,z') \right] \\ &= \frac{1}{A \sigma_{in}^{VN}} \int d^2b \{ 1 - \exp[-\sigma_{in}^{VN} T(b)] \} \\ &= \frac{\sigma_{in}^{VA}}{A \sigma_{in}^{VN}}. \end{aligned} \tag{3}$$

Here z is the longitudinal coordinate and $\vec{b}$ is the impact parameter of the production point of vector meson. In Eq. (3) $\rho_A(b,z)$ is the nuclear density and σ_{in}^{VN} is the inelastic V-N cross section.

(ii) In the limit of long l_c the expression for nuclear transparency takes a different form,

$$\mathrm{Tr}_A^{inc}|_{l_c \gg R_A} = \int d^2b\, T_A(b) \exp[-\sigma_{in}^{VN} T_A(b)], \tag{4}$$

where we assume $\sigma_{el}^{VN} \ll \sigma_{in}^{VN}$ for the sake of simplicity. $T_A(b)$ is the nuclear thickness function

$$T_A(b) = \int_{-\infty}^{\infty} dz\, \rho_A(b,z). \tag{5}$$

The exact expression that interpolates between the two regimes, Eqs. (3) and (4), can be found in Ref. [12].

The problem of CT-CL separation arises especially in production of light vector mesons (ρ^0, Φ^0) [10]. In this case the coherence and formation lengths are comparable starting from the photoproduction limit up to $Q^2 \sim 1$–2 GeV^2. In charmonium production, however, there is a strong inequality $l_f > l_c$ independent of Q^2 and ν. It leads to a different scenario of CT-CL mixing compared to light vector meson production. This fact gives a motivation for separate study of J/Ψ production presented in this paper using light-cone dipole approach generalized for the case of a finite coherence length and developed in Ref. [10]. Another reason is supported by the recent paper [11], where charmonium production was calculated in the approximation of long coherence length $l_c \gg R_A$ using realistic charmonium wave functions from Ref. [13] and corrections for finite values of l_c. It gives very interesting possibility to compare the predictions of the present paper with the results obtained from Ref. [11] for enhancement of reliability of theoretical predictions as a realistic basis for planned future electron-nucleus collisions.

The paper is organized as follows. In Sec. II we present a short review of the light-cone (LC) approach to diffractive electroproduction of vector mesons in the rest frame of the nucleon target. Here we also present the following individual ingredients contained in the production amplitude.

(i) The dipole cross section characterizing the universal interaction cross section for a colorless quark-antiquark dipole and a nucleon.

(ii) The LC wave function for a quark-antiquark fluctuation of the virtual photon.

(iii) The LC wave function of charmonia.

As the first test of the model we calculate in Sec. III the cross section of elastic electroproduction of J/Ψ off a nucleon target. Model calculations reproduce both energy and Q^2 dependence remarkably well, including the absolute normalization.

Section IV is devoted to incoherent production of J/Ψ off nuclei. Model predictions are compared with the data of the New Muon Collaboration (NMC) on the Sn/C ratio of nuclear transparencies as a function of the photon energy. We find a different scenario of an interplay between coherence and formation length effects from that occurring in light vector meson production. Because a variation of l_c with Q^2 can mimic CT at medium and low energies, one can map experimental events in Q^2 and ν in such a way as to keep $l_c = \mathrm{const}$. The LC dipole formalism predicts rather large effect of CT in the range of $Q^2 \leqslant 20$ GeV^2. This fact makes it feasible to find a clear signal of CT effects also in exclusive production of J/Ψ in the planned future experiments.

Coherent production of vector mesons off nuclei leaving the nucleus intact is studied in Sec. V. The detailed calculations show that the effect of CT on the Q^2 dependence of nuclear transparency at $l_c = \mathrm{const}$ is weaker than in the case of incoherent production and is difficult to be detected at low energies since the cross section is small.

We show that the gluon shadowing suppresses electroproduction of charmonia at high energies. However, it is not very significant in the energy range important for search of CT effects. Despite this fact, we include the gluon shadowing effects in all calculations for nuclear transparency.

The results of the paper are summarized and discussed in Sec. VI. An optimistic prognosis for discovery of CT in electroproduction of charmonia is made for the future experiments.

II. A SHORT REVIEW OF THE LIGHT-CONE DIPOLE PHENOMENOLOGY FOR ELASTIC ELECTROPRODUCTION OF CHARMONIA $\gamma^* N \to J/\Psi\ N$

The LC dipole approach for elastic electroproduction $\gamma^* N \to VN$ was already used in Ref. [13] to study the exclusive photo- and electroproduction of charmonia and in Ref. [10] for elastic virtual photoproduction of light vector mesons ρ^0 and Φ^0. Therefore, we present only a short review of this LC phenomenology with the main emphasis on elastic electroproduction of charmonia. Here a diffractive process is treated as elastic scattering of a $\bar{q}q$ fluctuation ($\bar{c}c$ fluctuation for the case of charmonium production) of the incident particle. The elastic amplitude is given by convolution of the universal flavor independent dipole cross section for the $\bar{q}q$ interaction with a nucleon, σ_{qq}^{-}, [3] and the initial and final wave functions. For the exclusive photo- or electroproduction of charmonia $\gamma^* N \to J/\Psi\ N$ the forward production amplitude is represented in the quantum-mechanical form,

$$\mathcal{M}_{\gamma^* N \to J/\Psi N}(s,Q^2) = \langle J/\Psi | \sigma_{qq}^{N}(\vec{r},s) | \gamma^* \rangle = \int_0^1 d\alpha \int d^2 r \Psi^*_{J/\Psi}(\vec{r},\alpha) \times \sigma_{qq}^{-}(\vec{r},s) \Psi_{\bar{c}c}^{-}(\vec{r},\alpha,Q^2), \quad (6)$$

with the normalization

$$\left.\frac{d\sigma}{dt}\right|_{t=0} = \frac{|\mathcal{M}|^2}{16\pi}. \quad (7)$$

In order to calculate the photoproduction amplitude one needs to know the following ingredients of Eq. (6).

(i) The dipole cross section $\sigma_{qq}^{-}(\vec{r},s)$ which depends on the $\bar{q}q$ transverse separation $\vec{r}$ and the c.m. energy squared s.

(ii) The LC wave function of the $\bar{c}c$ Fock component of the photon $\Psi_{\bar{c}c}^{-}(\vec{r},\alpha,Q^2)$, which also depends on the photon virtuality Q^2 and the relative share α of the photon momentum carried by the quark.

(iii) The LC wave function $\Psi_{J/\Psi}(\vec{r},\alpha)$ of J/Ψ.

Note that in the LC formalism the photon and meson wave functions contain also higher Fock states $|\bar{q}q\rangle$, $|\bar{q}qG\rangle$, $|\bar{q}q2G\rangle$, etc. The effects of higher Fock states are implicitly incorporated into the energy dependence of the dipole cross section $\sigma_{qq}^{-}(\vec{r},s)$ as is given in Eq. (6).

The dipole cross section $\sigma_{qq}^{-}(\vec{r},s)$ represents the interaction of a $\bar{q}q$ dipole of transverse separation $\vec{r}$ with a nucleon [3]. It is a flavor independent universal function of $\vec{r}$ and energy and allows to describe various high-energy processes in an uniform way. It is known to vanish quadratically $\sigma_{qq}^{-}(r,s) \propto r^2$ as $r \to 0$ due to color screening (CT property) and cannot be predicted reliably because of poorly known higher-order perturbative QCD (pQCD) corrections and nonperturbative effects. A detailed discussion about the dipole cross section $\sigma_{qq}^{-}(\vec{r},s)$ with an emphasis on the production of light vector mesons is presented in Ref. [10]. In electroproduction of charmonia the corresponding transverse separations of $\bar{c}c$ dipole reach the values $\leqslant 0.4$ fm (semiperturbative region). It means that nonperturbative effects are sufficiently smaller as compared to light vector mesons. Similarly, the relativistic corrections are also small enough and the nonrelativistic limit $\alpha = 0.5$ can be safely used with rather high accuracy [8].

There are two popular parametrizations of $\sigma_{qq}^{-}(\vec{r},s)$. The first one suggested in Ref. [14] reflects the fact that at small separations the dipole cross section should be a function of r and $x_{Bj} \sim 1/(r^2 s)$ to reproduce Bjorken scaling. It describes well the data for deep-inelastic scattering (DIS) at small x_{Bj} and medium and high Q^2. However, at small Q^2 it cannot be correct since it predicts energy independent hadronic cross sections. Besides, x_{Bj} is not anymore a proper variable at small Q^2 and should be replaced by energy. This defect is removed by the second parametrization suggested in Ref. [15], which is similar to the one in Ref. [14], but contains an explicit energy dependence. It is valid down to the limit of real photoproduction. Since we want to study CT effects starting from $Q^2 = 0$, we choose the second parametrization, which has the following form:

$$\sigma_{qq}^{-}(r,s) = \sigma_0(s)[1 - e^{-r^2/r_0^2(s)}], \quad (8)$$

where

$$\sigma_0(s) = \sigma_{tot}^{\pi p}(s)\left[1 + \frac{3}{8}\frac{r_0^2(s)}{\langle r_{ch}^2 \rangle}\right] \text{ mb} \quad (9)$$

and

$$r_0(s) = 0.88\left(\frac{s}{s_0}\right)^{-0.14} \text{ fm}. \quad (10)$$

Here $\langle r_{ch}^2 \rangle = 0.44$ fm^2 is the mean pion charge radius squared; $s_0 = 1000$ GeV^2. The cross section $\sigma_{tot}^{\pi p}(s)$ was fitted to data in Refs. [16,17],

$$\sigma_{tot}^{\pi p}(s) = 23.6\left(\frac{s}{s_0}\right)^{0.079} \text{ mb}. \quad (11)$$

The dipole cross section, Eqs. (8)–(11), provides the imaginary part of the elastic amplitude. It is known, however, that the energy dependence of the total cross section generates also a real part [18],

$$\sigma_{qq}^{-}(r,s) \Rightarrow \left(1 - i\frac{\pi}{2}\frac{\partial}{\partial \ln(s)}\right)\sigma_{qq}^{-}(r,s). \quad (12)$$

The energy dependence of the dipole cross section Eq. (8) is rather steep at small r, leading to a large real part which should not be neglected. For instance, the photoproduction amplitude of the process $\gamma N \to J/\Psi N$ rises $\propto s^{0.2}$ and the real-to-imaginary part ratio is over 30%.

Although the calculations of DIS using parametrization of the dipole cross section, Eq. (8), successfully describe the data at small x_{Bj} up to $Q^2 \approx 10$ GeV^2, we prefer this parametrization for study of charmonium electroproduction. The

reason is that we want to study CT effects predominantly in the range of $Q^2 \leqslant 20$ GeV^2 and, in addition, parametrization Eq. (8) describes the transition toward photoproduction limit better than the parametrization presented in Ref. [14]. Besides, in the paper [13] it was shown by studying electroproduction of charmonia off nucleons that the difference between the predictions using both parametrizations [14] and Eq. (8) is rather small and can be taken as a measure of the theoretical uncertainty.

The perturbative distribution amplitude ("wave function") of the $\bar{q}q$ ($\bar{c}c$ for J/Ψ production) Fock component of the photon has the following form for transversely (T) and longitudinally (L) polarized photons [19–21]:

$$\Psi_{\bar{q}q}^{T,L}(\vec{r},\alpha)=\frac{\sqrt{N_C\alpha_{em}}}{2\pi}Z_q\bar{\chi}\hat{O}^{T,L}\chi K_0(\epsilon r), \tag{13}$$

where χ and $\bar{\chi}$ are the spinors of the quark and antiquark, respectively; Z_q is the quark charge, $Z_q=Z_c=2/3$ for J/Ψ production; $N_C=3$ is the number of colors. $K_0(\epsilon r)$ is a modified Bessel function with

$$\epsilon^2=\alpha(1-\alpha)Q^2+m_c^2, \tag{14}$$

where $m_c=1.5$ GeV is mass of the c quark, and α is the fraction of the LC momentum of the photon carried by the quark. The operators $\hat{O}^{T,L}$ read

$$\hat{O}^T=m_c\vec{\sigma}\cdot\vec{e}+i(1-2\alpha)(\vec{\sigma}\cdot\vec{n})(\vec{e}\cdot\vec{\nabla}_r)+(\vec{\sigma}\times\vec{e})\cdot\vec{\nabla}_r, \tag{15}$$

$$\hat{O}^L=2Q\alpha(1-\alpha)(\vec{\sigma}\cdot\vec{n}). \tag{16}$$

Here $\vec{\nabla}_r$ acts on transverse coordinate $\vec{r}$; $\vec{e}$ is the polarization vector of the photon, $\vec{n}$ is a unit vector parallel to the photon momentum, and $\vec{\sigma}$ is the three vector of the Pauli spin matrices.

In general, the transverse $\bar{q}q$ separation is controlled by the distribution amplitude, Eq. (13), with the mean value

$$\langle r\rangle\sim\frac{1}{\epsilon}=\frac{1}{\sqrt{Q^2\alpha(1-\alpha)+m_q^2}}. \tag{17}$$

For production of light vector meson very asymmetric $\bar{q}q$ pairs with α or $(1-\alpha)\lesssim m_q^2/Q^2$ become possible. Consequently, the mean transverse separation $\langle r\rangle\sim 1/m_q$ becomes huge since one must use current quark masses within PQCD. However, that is not the case in charmonium production because of a large quark mass $m_c=1.5$ GeV. Therefore, we are out of the problem how to include nonperturbative interaction effects between c and $\bar{c}$ because they are rather small. Despite this fact, for completeness we include these nonperturbative interaction effects in all calculations to avoid small but supplementary uncertainties in predictions. We take from Ref. [15] the corresponding phenomenology including the interaction between c and $\bar{c}$ based on the light-cone Green function approach.

The Green function $G_{\bar{q}q}(z_1,\vec{r}_1;z_2,\vec{r}_2)$ describes the propagation of an interacting $\bar{q}q$ pair ($\bar{c}c$ pair for the case of J/Ψ production) between points with longitudinal coordinates z_1 and z_2 and with initial and final separations $\vec{r}_1$ and $\vec{r}_2$. This Green function satisfies the two-dimensional Schrödinger equation,

$$\begin{aligned} i\frac{d}{dz_2}&G_{\bar{q}q}(z_1,\vec{r}_1;z_2,\vec{r}_2)\\ &=\left[\frac{\epsilon^2-\Delta_{r_2}}{2\nu\alpha(1-\alpha)}+V_{\bar{q}q}(z_2,\vec{r}_2,\alpha)\right]\\ &\times G_{\bar{q}q}(z_1,\vec{r}_1;z_2,\vec{r}_2). \end{aligned} \tag{18}$$

Here ν is the photon energy. The Laplacian Δ_r acts on the coordinate r.

The imaginary part of the LC potential $V_{\bar{q}q}(z_2,\vec{r}_2,\alpha)$ in Eq. (18) is responsible for attenuation of the $\bar{q}q$ in the medium, while the real part represents the interaction between q and $\bar{q}$. This potential is supposed to provide the correct LC wave functions of vector mesons. For the sake of simplicity we use the oscillator form of the potential,

$$\mathrm{Re}\,V_{\bar{q}q}(z_2,\vec{r}_2,\alpha)=\frac{a^4(\alpha)\vec{r}_2^2}{2\nu\alpha(1-\alpha)}, \tag{19}$$

which leads to a Gaussian r dependence of the LC wave function of the meson ground state. The shape of the function $a(\alpha)$ will be discussed below.

In this case, Eq. (18) has an analytical solution, the harmonic oscillator Green function [22],

$$\begin{aligned} G_{\bar{q}q}&(z_1,\vec{r}_1;z_2,\vec{r}_2)\\ &=\frac{a^2(\alpha)}{2\pi i\sin(\omega\Delta z)}\exp\left\{\frac{ia^2(\alpha)}{\sin(\omega\Delta z)}[(r_1^2+r_2^2)\cos(\omega\Delta z)\right.\\ &\left.-2\vec{r}_1\cdot\vec{r}_2]\right\}\exp\left[-\frac{i\epsilon^2\Delta z}{2\nu\alpha(1-\alpha)}\right], \end{aligned} \tag{20}$$

where $\Delta z=z_2-z_1$ and

$$\omega=\frac{a^2(\alpha)}{\nu\alpha(1-\alpha)}. \tag{21}$$

The boundary condition is $G_{\bar{q}q}(z_1,\vec{r}_1;z_2,\vec{r}_2)|_{z_2=z_1}=\delta^2(\vec{r}_1-\vec{r}_2)$.

The probability amplitude to find the $\bar{q}q$ fluctuation of a photon at the point z_2 with separation $\vec{r}$ is given by an integral over the point z_1, where the $\bar{q}q$ is created by the photon with initial zero separation,

$$\Psi^{T,L}_{qq}(\vec{r},\alpha)=\frac{iZ_q\sqrt{\alpha_{em}}}{4\pi\nu\alpha(1-\alpha)}\int_{-\infty}^{z_2}dz_1 \times(\bar{\chi}\hat{O}^{T,L}\chi)G^{-}_{qq}(z_1,\vec{r}_1;z_2,\vec{r})|_{r_1=0}. \quad (22)$$

The operators $\hat{O}^{T,L}$ are defined in Eqs. (15) and (16). Here they act on the coordinate $\vec{r}_1$.

If we write the transverse part as

$$\bar{\chi}\hat{O}^T\chi=\bar{\chi}m_c\vec{\sigma}\cdot\vec{e}\chi+\bar{\chi}[i(1-2\alpha)(\vec{\sigma}\cdot\vec{n})\vec{e} +(\vec{\sigma}\times\vec{e})]\chi\cdot\vec{\nabla}_r =E+\vec{F}\cdot\vec{\nabla}_r, \quad (23)$$

then the distribution functions read

$$\Psi^{T}_{qq}(\vec{r},\alpha)=Z_q\sqrt{\alpha_{em}}[E\Phi_0(\epsilon,r,\lambda)+\vec{F}\cdot\vec{\Phi}_1(\epsilon,r,\lambda)], \quad (24)$$

$$\Psi^{L}_{qq}(\vec{r},\alpha)=2Z_q\sqrt{\alpha_{em}}Q\alpha(1-\alpha)\bar{\chi}\vec{\sigma}\cdot\vec{n}\chi\Phi_0(\epsilon,r,\lambda), \quad (25)$$

where

$$\lambda=\frac{2a^2(\alpha)}{\epsilon^2}. \quad (26)$$

The functions $\Phi_{0,1}$ in Eqs. (24) and (25) are defined as

$$\Phi_0(\epsilon,r,\lambda)=\frac{1}{4\pi}\int_0^\infty dt\frac{\lambda}{\mathrm{sh}(\lambda t)}\exp\left[-\frac{\lambda\epsilon^2r^2}{4}\mathrm{cth}(\lambda t)-t\right], \quad (27)$$

$$\vec{\Phi}_1(\epsilon,r,\lambda)=\frac{\epsilon^2\vec{r}}{8\pi}\int_0^\infty dt\left[\frac{\lambda}{\mathrm{sh}(\lambda t)}\right]^2\exp\left[-\frac{\lambda\epsilon^2r^2}{4}\mathrm{cth}(\lambda t)-t\right], \quad (28)$$

where $\mathrm{sh}(x)$ and $\mathrm{cth}(x)$ is the hyperbolic sine and hyperbolic cotangent, respectively. Note that the $\bar{q}$-q interaction enters Eqs. (24) and (25) via the parameter λ defined in Eq. (26). In the limit of vanishing interaction $\lambda\to 0$ (i.e., $Q^2\to\infty$, α is fixed, $\alpha\neq 0$ or 1) Eqs. (24) and (25) produce the perturbative expressions of Eq. (13). As mentioned above, for charmonium production nonperturbative interaction effects are quite weak. Consequently, the parameter λ (26) is rather small due to a large mass of the c quark.

With the choice $a^2(\alpha)\propto\alpha(1-\alpha)$ the end-point behavior of the mean square interquark separation $\langle r^2\rangle\propto 1/\alpha(1-\alpha)$ contradicts the idea of confinement. Following Ref. [15] we fix this problem via a simple modification of the LC potential,

$$a^2(\alpha)=a_0^2+4a_1^2\alpha(1-\alpha). \quad (29)$$

The parameters a_0 and a_1 were adjusted in Ref. [15] to the data on total photoabsorption cross section [23,24], diffractive photon dissociation, and shadowing in nuclear photoabsorption reaction. The results of our calculations vary within 1% only when a_0 and a_1 satisfy the relation

$$a_0^2=v^{1.15}(0.112)^2\ \ \mathrm{GeV}^2,$$
$$a_1^2=(1-v)^{1.15}(0.165)^2\ \ \mathrm{GeV}^2, \quad (30)$$

where v takes any value $0\leqslant v\leqslant 1$. In the view of this insensitivity of the observables we fix the parameters at $v=1/2$. We checked that this choice does not affect our results beyond a few percent uncertainty.

The last ingredient in elastic production amplitude (6) is the charmonium wave function. We use a popular prescription [25] applying the Lorentz boost to the rest frame wave function assumed to be Gaussian, which leads to radial parts of transversely and longitudinally polarized mesons in the form

$$\Phi^{T,L}_{J/\Psi}(\vec{r},\alpha)=C^{T,L}_{J/\Psi}\alpha(1-\alpha)f(\alpha)\exp\left[-\frac{\alpha(1-\alpha)r^2}{2R^2}\right] \quad (31)$$

with a normalization defined below, and

$$f(\alpha)=\exp\left[-\frac{m_c^2R^2}{2\alpha(1-\alpha)}\right] \quad (32)$$

with the parameters from Ref. [26], $R=0.183$ fm and $m_c=1.5$ GeV. A detailed analysis of various problems in this relativization procedure [27] leads to the same form as Eq. (31).

We assume that the distribution amplitudes of $\bar{c}c$ fluctuations for J/Ψ and for the photon have a similar structure [26]. Then in analogy to Eqs. (24) and (25),

$$\Psi^{T}_{J/\Psi}(\vec{r},\alpha)=(E+\vec{F}\cdot\vec{\nabla}_r)\Phi^{T}_{J/\Psi}(\vec{r},\alpha), \quad (33)$$

$$\Psi^{L}_{J/\Psi}(\vec{r},\alpha)=2m_{J/\Psi}\alpha(1-\alpha)(\bar{\chi}\vec{\sigma}\cdot\vec{n}\chi)\Phi^{L}_{J/\Psi}(\vec{r},\alpha). \quad (34)$$

Correspondingly, the normalization conditions for the transverse and longitudinal charmonium wave functions read

$$N_C\int d^2r\int d\alpha\{m_c^2|\Phi^{T}_{J/\Psi}(\vec{r},\alpha)|^2 +[\alpha^2+(1-\alpha)^2]|\partial_r\Phi^{T}_{J/\Psi}(\vec{r},\alpha)|^2\} =1, \quad (35)$$

$$4N_C\int d^2r\int d\alpha\,\alpha^2(1-\alpha)^2m_{J/\Psi}^2|\Phi^{L}_{J/\Psi}(\vec{r},\alpha)|^2=1. \quad (36)$$

III. ELECTROPRODUCTION OF J/Ψ ON A NUCLEON, COMPARISON WITH DATA

In this section we verify first the LC approach by comparing with data for nucleon target. The forward production amplitude $\gamma^*N\to J/\Psi N$ for transverse and longitudinal pho-

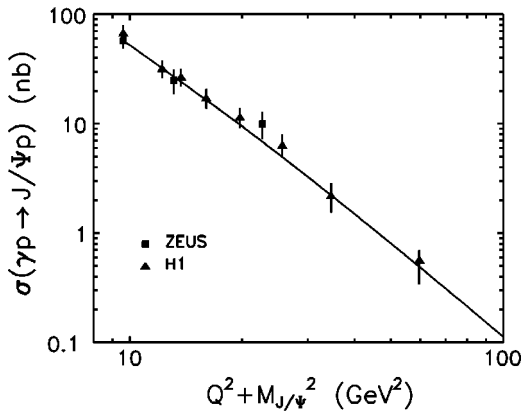

FIG. 1. $Q^2+m_{J/\Psi}^2$ dependence of the integrated cross section for the reactions $\gamma^* p \to J/\Psi p$. The model calculations are compared with H1 [29] and ZEUS [30] data at energy $W=90$ GeV.

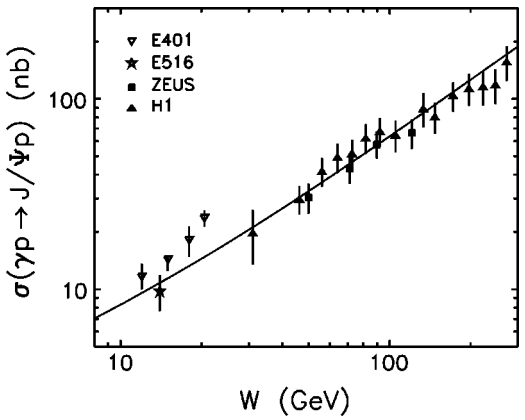

FIG. 2. Energy dependence of the real photoproduction cross section on a nucleon, $\gamma p \to J/\Psi p$. Our results are compared with data from the fixed target E401 [31], E516 [32], and collider HERA H1 [28] and ZEUS [33] experiments.

tons and charmonium is calculated using the nonperturbative photon, Eqs. (24) and (25), and vector meson, Eqs. (33), (34), wave functions and has the following form:

$$\mathcal{M}^T_{\gamma^* N\to J/\Psi N}(s,Q^2)\big|_{t=0} = N_C Z_c \sqrt{2\ \alpha_{em}} \int d^2r\, \sigma_{qq}(\vec{r},s) \times \int_0^1 d\alpha \{ m_c^2 \Phi_0(\epsilon,\vec{r},\lambda)\Phi^T_{J/\Psi}(\vec{r},\alpha) - [\alpha^2+(1-\alpha)^2]\vec{\Phi}_1(\epsilon,\vec{r},\lambda)\cdot\vec{\nabla}_r \Phi^T_{J/\Psi}(\vec{r},\alpha)\}, \tag{37}$$

$$\mathcal{M}^L_{\gamma^* N\to J/\Psi N}(s,Q^2)\big|_{t=0} = 4N_C Z_c \sqrt{2\ \alpha_{em}} m_{J/\Psi} Q \int d^2r\, \sigma_{qq}(\vec{r},s) \int_0^1 d\alpha\, \alpha^2 \times (1-\alpha)^2 \Phi_0(\epsilon,\vec{r},\lambda)\Phi^L_{J/\Psi}(\vec{r},\alpha). \tag{38}$$

These amplitudes are normalized as $|\mathcal{M}^{T,L}|^2 = 16\pi d\sigma_N^{T,L}/dt|_{t=0}$. The real part of the amplitude is included according to the prescription described in the preceding section. We calculate the cross sections $\sigma=\sigma^T+\epsilon'\sigma^L$ assuming that the photon polarization is $\epsilon'=1$.

Now we can check the absolute value of the production cross section by comparing with data for elastic charmonium electroproduction $\gamma^* p \to J/\Psi p$. Unfortunately, data are available only for the cross section integrated over t,

$$\sigma^{T,L}(\gamma^* N\to J/\Psi\ N) = \frac{|\mathcal{M}^{T,L}|^2}{16\pi B_{J/\Psi}}, \tag{39}$$

where $B_{J/\Psi}$ is the slope parameter in reaction $\gamma^* N \to J/\Psi N$. We use the experimental value [28] $B_{J/\Psi}=4.7\ \mathrm{GeV}^{-2}$.

Our predictions are plotted in Fig. 1, together with the data on the $Q^2+m_{J/\Psi}^2$ dependence of the cross section from H1 [29] and ZEUS [30].

The second test of our approach is a description of the real J/Ψ photoproduction. As we discussed in the preceding section, we include for completeness into calculations the nonperturbative interaction effects between c and $\bar{c}$ although they are rather small. Comparison of the model with data [31,32,28,33] for the energy dependence of the cross section of real J/Ψ photoproduction is presented in Fig. 2.

The normalization of the cross section and its energy and Q^2 dependence are remarkably well reproduced in Figs. 1 and 2. This is an important achievement since the absolute normalization is usually much more difficult to reproduce the production cross sections than nuclear effects. For instance, the similar, but simplified calculations in Ref. [8] underestimate the J/Ψ photoproduction cross section on protons by an order of magnitude.

As a cross check for the choice of the J/Ψ wave function in Eqs. (31) and (32) we also calculated the total J/Ψ nucleon cross section, which was already estimated in Ref. [13] using the charmonium wave functions calculated with several realistic $\bar{q}q$ potentials. The J/Ψ nucleon total cross section has the form

$$\sigma_{tot}^{J/\Psi-N} = N_C \int d^2r \int d\alpha \{ m_c^2 |\Phi^T_{J/\Psi}(\vec{r},\alpha)|^2 + [\alpha^2+(1-\alpha)^2]|\partial_r \Phi^T_{J/\Psi}(\vec{r},\alpha)|^2\}\sigma_{qq}(\vec{r},s). \tag{40}$$

We calculated $\sigma_{tot}^{J/\Psi-N}$ with the charmonium wave function in the form (31) (corresponding to quadratic $\bar{q}$-q potential) with the parameters described in the preceding section. For the dipole cross section we adopt the parametrization (8) which is designed to describe low-Q^2 data. Then, at $\sqrt{s}=10$ GeV we obtain $\sigma_{tot}^{J/\Psi-N}=4.2$ mb, which is not in contradiction with $\sigma_{tot}^{J/\Psi-N}=3.6\pm0.1$ mb evaluated in Ref. [13] using more realistic $\bar{q}$-q potentials and/or charmonium wave functions.

IV. INCOHERENT PRODUCTION OF CHARMONIA OFF NUCLEI

A. The *LC* Green function formalism

In this section we present a short review of the LC Green function formalism for incoherent production of an arbitrary vector meson. For the case of charmonium production one should replace $V\to J/\Psi$ and $\bar{q}q\to\bar{c}c$. In general, the diffractive incoherent (quasielastic) production of vector mesons off nuclei, $\gamma^*A\to VX$, is associated with a breakup of the nucleus, but without production of new particles. In other words, one sums over all final states of the target nucleus except those which contain particle (pion) creation. The observable usually studied experimentally is nuclear transparency defined as

$$\mathrm{Tr}_A^{inc}=\frac{\sigma^{inc}_{\gamma^*A\to VX}}{A\sigma_{\gamma^*N\to VN}}. \tag{41}$$

The t slope of the differential quasielastic cross section is the same as on a nucleon target. Therefore, instead of integrated cross sections one can also use nuclear transparency expressed via the forward differential cross sections Eq. (7),

$$\mathrm{Tr}_A^{inc}=\frac{1}{A}\left|\frac{\mathcal{M}_{\gamma^*A\to VX}(s,Q^2)}{\mathcal{M}_{\gamma^*N\to VN}(s,Q^2)}\right|^2. \tag{42}$$

In the LC Green function approach [10] the physical photon $|\gamma^*\rangle$ is decomposed into different Fock states, namely, the bare photon $|\gamma^*\rangle_0$, $|\bar{q}q\rangle$, $|\bar{q}qG\rangle$, etc. As we mentioned above, the higher Fock states containing gluons describe the energy dependence of the photoproduction reaction on a nucleon. Besides, those Fock components also lead to gluon shadowing as far as nuclear effects are concerned. However, these fluctuations are heavier and have a shorter coherence time (lifetime) than the lowest $|\bar{q}q\rangle$ state. Therefore, at medium energies only $|\bar{q}q\rangle$ fluctuations of the photon matter. Consequently, gluon shadowing related to the higher Fock states will be dominated at high energies. Detailed description and calculation of gluon shadowing for the case of vector meson production off nuclei is presented in Refs. [10,11]. Although the gluon shadowing effects are rather small in the kinematic range important for study of CT effects in elastic and quasielastic charmonium production off nuclei, we include them in all calculations.

Propagation of an interacting $\bar{q}q$ pair in a nuclear medium is also described by the Green function satisfying the evolution Eq. (18). However, the potential in this case acquires an imaginary part which represents absorption in the medium,

$$\mathrm{Im}\,V^-_{qq}(z_2,\vec{r},\alpha)=-\frac{\sigma^-_{qq}(\vec{r},s)}{2}\rho_A(b,z_2), \tag{43}$$

where $\rho_A(b,z_2)$ is the nuclear density function defined at the point with longitudinal coordinate z_2 and impact parameter $\vec{b}$. The evolution equation (18) with the potential $V^-_{qq}(z_2,\vec{r}_2,\alpha)$ containing this imaginary part was used in Refs. [34,35], and nuclear shadowing in deep-inelastic scattering was calculated in good agreement with data.

The analytical solution of Eq. (20) is only known for the harmonic oscillator potential $V(r)\propto r^2$. To keep the calculations reasonably simple we are forced to use the dipole approximation,

$$\sigma^-_{qq}(r,s)=C(s)r^2, \tag{44}$$

which allows to obtain the Green function in an analytical form.

The energy dependent factor $C(s)$ in Eq. (44) is adjusted by demanding that calculations employing the approximation Eq. (44) reproduce correctly the results based on the realistic cross section Eq. (8) in the limit $l_c\gg R_A$ (the so called ''frozen'' approximation) when the Green function takes the simple form,

$$G^-_{qq}(z_1,\vec{r}_1;z_2,\vec{r}_2)\Rightarrow\delta(\vec{r}_1-\vec{r}_2)\exp\left[-\frac{1}{2}\sigma^-_{qq}(r_1)\int_{z_1}^{z_2}dz\,\rho_A(b,z)\right], \tag{45}$$

where the dependence of the Green function on impact parameter is dropped. Thus, for incoherent production of vector mesons, the factor $C(s)$ is fixed by the relation

$$\frac{\int d^2bT_A(b)\left|\int d^2rr^2\exp\left[-\frac{1}{2}C(s)r^2T_A(b)\right]\int d\alpha\Psi_V^{*T,L}(\vec{r},\alpha)\Psi^{T,L}_{\bar{q}q}(\vec{r},\alpha)\right|^2}{\left|\int d^2r\,r^2\int d\alpha\Psi_V^{*T,L}(\vec{r},\alpha)\Psi^{T,L}_{\bar{q}q}(\vec{r},\alpha)\right|^2}$$
$$=\frac{\int d^2bT_A(b)\left|\int d^2r\,\sigma^-_{qq}(r,s)\exp\left[-\frac{1}{2}\sigma^-_{qq}(r,s)T_A(b)\right]\int d\alpha\Psi_V^{*T,L}(\vec{r},\alpha)\Psi^{T,L}_{\bar{q}q}(\vec{r},\alpha)\right|^2}{\left|\int d^2r\,\sigma^-_{qq}(r,s)\int d\alpha\,\Psi_V^{*T,L}(\vec{r},\alpha)\Psi^{T,L}_{\bar{q}q}(\vec{r},\alpha)\right|^2} \tag{46}$$

To take advantage of the analytical form of the Green function which is known only for the LC potential Eq. (43) with a constant nuclear density, we use the approximation $\rho_A(b,z)=\rho_0\Theta(R_A^2-b^2-z^2)$. Therefore we have to use this form for Eq. (46) as well. The value of the mean nuclear density ρ_0 was determined using the relation

$$\int d^2b[1-\exp(-\sigma_0\rho_0\sqrt{R_A^2-b^2})] = \int d^2b\left[1-\exp\left(-\frac{\sigma_0}{2}T(b)\right)\right], \quad (47)$$

where the nuclear thickness function $T_A(b)$ is calculated with the realistic Woods-Saxon form of the nuclear density. The value of ρ_0 turns out to be practically independent of the cross section σ_0 in the range from 1 to 50 mb.

With the potential Eqs. (43) and (44) the solution of Eq. (18) has the same form as Eq. (20), except that one should replace $\omega\Rightarrow\Omega$ and $a^2(\alpha)\Rightarrow b(\alpha)$, where

$$\Omega=\frac{b(\alpha)}{\nu\alpha(1-\alpha)}=\frac{\sqrt{a^4(\alpha)-i\rho_A(b,z)\nu\alpha(1-\alpha)C(s)}}{\nu\alpha(1-\alpha)}. \quad (48)$$

As we discussed in Ref. [10] the value of l_c can distinguish different regimes of vector meson production.

(i) The CL is much shorter than the mean nucleon spacing in a nucleus ($l_c\to 0$). In this case $G(z_2,\vec{r}_2;z_1,\vec{r}_1)\to\delta(z_2-z_1)$. Correspondingly, the formation time of the meson wave function is very short as well as given in Eq. (1). For light vector mesons $l_f\sim l_c$ and since formation and coherence lengths are proportional to photon energy both must be short. Consequently, nuclear transparency is given by the simple formula Eq. (3) corresponding to the Glauber approximation.

(ii) In production of charmonia and other heavy flavor quarkonii there is a strong inequality $l_c<l_f$ and the intermediate case $l_c\to 0$, but $l_f\sim R_A$ can be realized. Then the formation of the meson wave function is described by the Green function and the numerator of the nuclear transparency ratio Eq. (42) has the form [8],

$$|\mathcal{M}_{\gamma^*A\to VX}(s,Q^2)|^2_{l_c\to 0;l_f\sim R_A} = \int d^2b\int_{-\infty}^{\infty}dz\,\rho_A(b,z)|F_1(b,z)|^2, \quad (49)$$

where

$$F_1(b,z)=\int_0^1 d\alpha\int d^2r_1d^2r_2\Psi_V^*(\vec{r}_2,\alpha)G(z',\vec{r}_2;z,\vec{r}_1) \times\sigma_{qq}^-(r_1,s)\Psi_{qq}^-(\vec{r}_1,\alpha)|_{z'\to\infty}. \quad (50)$$

(iii) In the high-energy limit $l_c\gg R_A$ (in fact, it is more correct to compare with the mean free path of the $\bar{q}q$ in a nuclear medium if the latter is shorter than the nuclear radius). In this case $G(z_2,\vec{r}_2;z_1,\vec{r}_1)\to\delta(\vec{r}_2-\vec{r}_1)$, i.e., all fluctuations of the transverse $\bar{q}q$ separation are ''frozen'' by Lorentz time dilation. Then, the numerator on the right-hand side of Eq. (42) takes the form [8],

$$|\mathcal{M}_{\gamma^*A\to VX}(s,Q^2)|^2_{l_c\gg R_A} = \int d^2b\,T_A(b)\left|\int d^2r\int_0^1 d\alpha\Psi_V^*(\vec{r},\alpha)\sigma_{qq}^-(r,s) \times\exp\left[-\frac{1}{2}\sigma_{qq}^-(r,s)T_A(b)\right]\Psi_{qq}^-(\vec{r},\alpha,Q^2)\right|^2. \quad (51)$$

In this case the $\bar{q}q$ attenuates with a constant absorption cross section like in the Glauber model, except that the whole exponential is averaged rather than just the cross section in the exponent. The difference between the results of the two prescriptions are the well known inelastic corrections of Gribov [3].

(iv) This regime reflects the general case when there is no restrictions for either l_c or l_f. The corresponding theoretical tool has been developed for the first time only recently in Ref. [10] and applied to electroproduction of light vector mesons at medium and high energies. Even within the VDM the Glauber model expression interpolating between the limiting cases of low [(i), (ii)] and high [(iii)] energies has been derived only recently [12] as well. In this general case the incoherent photoproduction amplitude is represented as a sum of two terms [36],

$$|\mathcal{M}_{\gamma^*A\to VX}(s,Q^2)|^2 = \int d^2b\int_{-\infty}^{\infty}dz\,\rho_A(b,z)|F_1(b,z)-F_2(b,z)|^2. \quad (52)$$

The first term $F_1(b,z)$ introduced above in Eq. (50) alone would correspond to the short l_c limit (ii). The second term $F_2(b,z)$ in Eq. (52) corresponds to the situation when the incident photon produces a $\bar{q}q$ pair diffractively and coherently at the point z_1 prior to incoherent quasielastic scattering at point z. The LC Green functions describe the evolution of the $\bar{q}q$ over the distance from z_1 to z and further on, up to the formation of the meson wave function. Correspondingly, this term has the form,

$$F_2(b,z)=\frac{1}{2}\int_{-\infty}^{z}dz_1\rho_A(b,z_1)\int_0^1 d\alpha\int d^2r_1d^2r_2d^2r \times\Psi_V^*(\vec{r}_2,\alpha)G(z'\to\infty,\vec{r}_2;z,\vec{r})\sigma_{qq}^-(\vec{r},s) \times G(z,\vec{r};z_1,\vec{r}_1)\sigma_{qq}^-(\vec{r}_1,s)\Psi_{qq}^-(\vec{r}_1,\alpha). \quad (53)$$

Equation (52) correctly reproduces the limits (i)–(iii). At $l_c\to 0$ the second term $F_2(b,z)$ vanishes because of strong oscillations, and Eq. (52) reproduces the Glauber expression Eq. (3). At $l_c\gg R_A$ the phase shift in the Green functions can be neglected and they acquire the simple form $G(z_2,\vec{r}_2;z_1,\vec{r}_1)\to\delta(\vec{r}_2-\vec{r}_1)$. In this case the integration over longitudinal coordinates in Eqs. (50) and (53) can be performed explicitly and the asymptotic expression Eq. (51) is recovered as well.

B. Comparison with data for incoherent production of J/Ψ

Exclusive incoherent electroproduction of vector mesons off nuclei has been suggested in Ref. [37] to be very convenient for investigation of CT. Increasing the photon virtuality Q^2, one squeezes the produced $\overline{qq}$ wave packet. Such a small colorless system propagates through the nucleus with little attenuation, provided that the energy is sufficiently high ($l_f \gg R_A$) so the fluctuations of the $\overline{qq}$ separation are frozen during propagation. Consequently, a rise of nuclear transparency $\mathrm{Tr}_A^{inc}(Q^2)$ with Q^2 should give a signal for CT. Indeed, such a rise was observed in the E665 experiment [38] at Fermilab for exclusive production of ρ^0 mesons off nuclei, what has been claimed as a manifestation of CT.

However, the effect of coherence length [39,12] leads also to a rise of $\mathrm{Tr}_A^{inc}(Q^2)$ with Q^2 and so can imitate CT effects. This happens when the coherence length varies from long to short [see Eq. (2)] compared to the nuclear size, and the length of the path in nuclear matter becomes shorter. Consequently, the vector meson (or $\overline{qq}$) attenuates less in nuclear medium. This happens when Q^2 increases at fixed ν. Therefore one should carefully disentangle these two phenomena.

Unfortunately, the data on charmonium electroproduction off nuclei are very scanty so far. There are only data from the NMC experiment [40] concerning energy dependence of the ratio of nuclear transparencies Tr_{Sn}^{inc} and Tr_C^{inc} for incoherent production of J/Ψ at $Q^2=0$. The corresponding photon energy varies from 60 to 210 GeV. It allows to study the transition from medium long to long coherence length, which varies from 2.4 to 8.5 fm. For long $l_c \gtrsim 8.5$ fm the ''frozen'' approximation can be used with high accuracy. In this case, nuclear transparency Tr_A^{inc} of incoherent (quasielastic) J/Ψ production can be calculated using Eq. (52) and the simplified ''frozen'' approximation Eqs. (45), (51). For medium long coherence length one cannot use the ''frozen'' approximation and fluctuations of the size of the $\overline{qq}$ pair become important. Because of a strong inequality $l_c < l_f$ for charmonium production CT effects are expected to be dominant at small and moderate energies. Consequently, they should lead to a rise with energy of Tr_A^{inc}. Such a scenario is depicted in Fig. 3 by solid and dashed curves. Dashed curve show our results using the LC Green function approach in the limit of short coherence length $l_c \to 0$, Eq. (49). The solid curve includes in addition also CL effects. Thus, the effect of coherence length manifest itself as a separation between the solid and dashed curves. Energy rise of the ratio $\mathrm{Tr}_{Sn}^{inc}/\mathrm{Tr}_C^{inc}$ at small and medium energy is a net manifestation of CT. It follows from the rise of formation time, see Eq. (1). At larger energies when CL effects also become important the $\mathrm{Tr}_{Sn}^{inc}/\mathrm{Tr}_C^{inc}$ ratio starts to fall down gradually.[2] Unfortunately, the NMC data have quite large error bars and therefore give only an indication for such a behavior. More accurate data

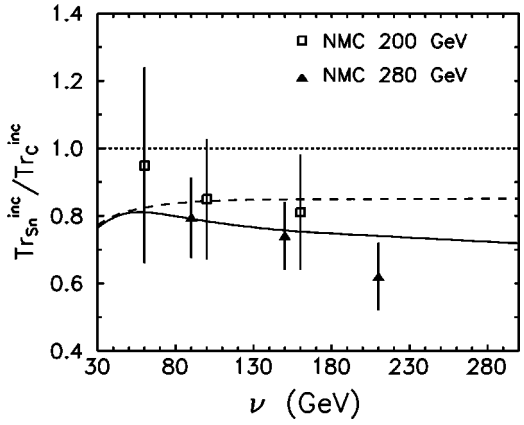

FIG. 3. Energy dependence of the ratio of nuclear transparencies Tr_{Sn} and Tr_C vs experimental points taken from the NMC experiment [40]. Solid and dashed curves show our results using the LC Green function approach in general case with no restriction for either l_c or l_f, Eq. (52), and in the limit of $l_c \to 0$, Eq. (49), respectively.

are needed for exploratory study of CT and CL effects. Charmonium real photoproduction off nuclei at small and large energies is very sensitive for investigation of CT and CL effect separately. However, it is not so for real photoproduction of light vector mesons when coherence and formation lengths are comparable and CT-CL mixing exists already at small energies.

Problem of separation of CT and CL effects was discussed in details in Ref. [10] with the main emphasis to light vector meson production where $l_c \gtrsim l_f$ at $Q^2 \lesssim 1-2$ GeV^2. In this paper we present the results for charmonium production, where a strong inequality $l_c < l_f$ in all discussed kinematic regions leads to a different scenario of CT-CL mixing compared to production of light vector mesons. Consequently, at fixed Q^2 and at small and medium energies the problem of CT-CL separation is not so acute. Besides, there is a prescription how to eliminate the effect of CL from the data on the Q^2 dependence of nuclear transparency [9]. One should simply bin the data in a way that keeps $l_c = \mathrm{const}$. It means that one should vary simultaneously ν and Q^2 maintaining the CL Eq. (2) constant,

$$\nu = \frac{1}{2} l_c (Q^2 + m_{J/\Psi}^2). \tag{54}$$

In this case the Glauber model predicts a Q^2 independent nuclear transparency, and any rise with Q^2 would signal CT [9].

The LC Green function technique incorporates both the effects of coherence and formation. We performed calculations of $\mathrm{Tr}_A^{inc}(Q^2)$ at fixed l_c starting from different minimal values of ν, which correspond to real photoproduction in Eq. (54),

$$\nu_{min} = \frac{1}{2} l_c m_{J/\Psi}^2 . \tag{55}$$

[2]In energy dependence of nuclear transparency at fixed Q^2, the effect of the coherence follows from variation of the coherence length from small to large values compared to the nuclear size, see Eq. (2).

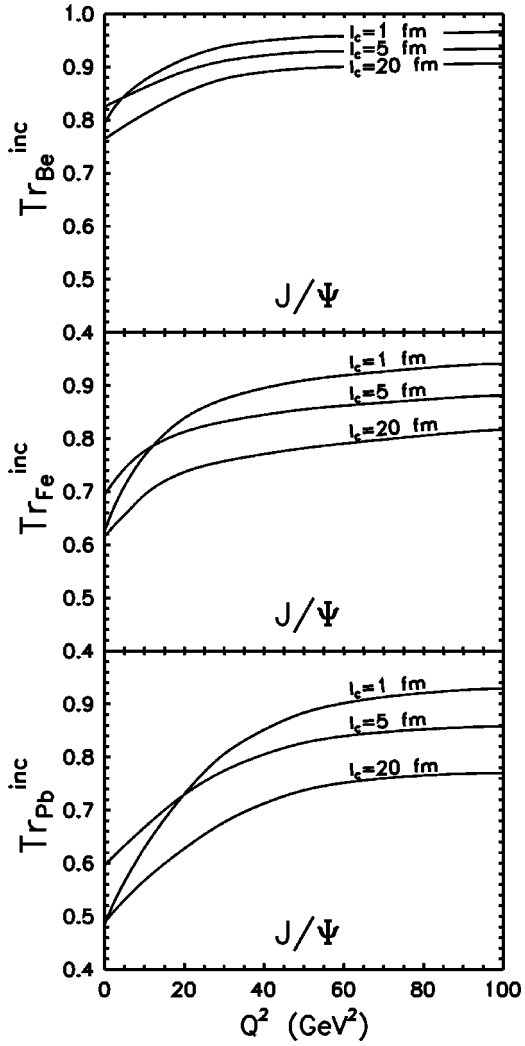

FIG. 4. Q^2 dependence of the nuclear transparency Tr_A^{inc} for exclusive electroproduction of J/Ψ on nuclear targets ^{9}Be, ^{56}Fe, and ^{207}Pb (from top to bottom). The CL is fixed at $l_c=1$, 5, and 20 fm.

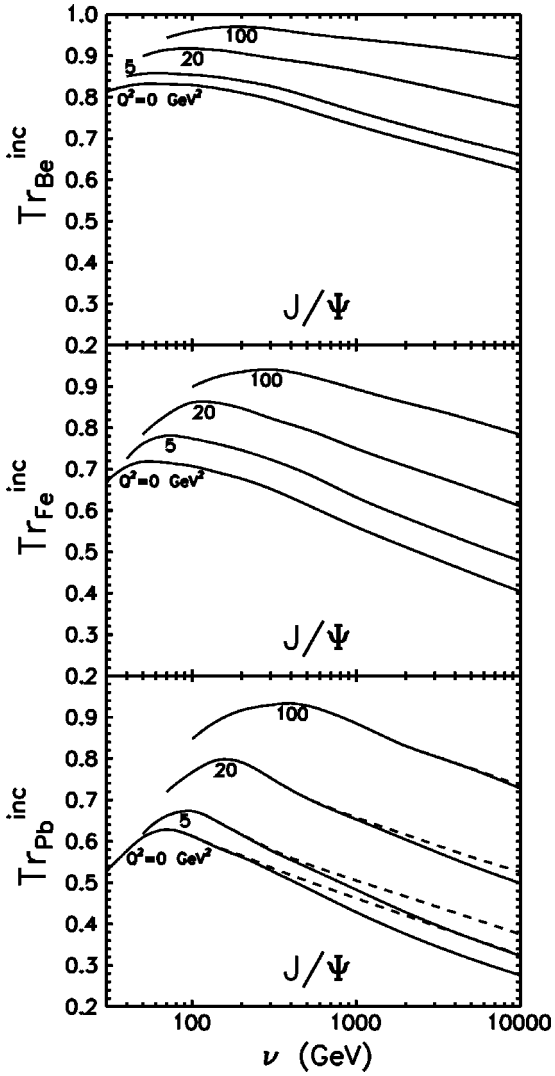

FIG. 5. Nuclear transparency for incoherent electroproduction $\gamma^*A\to J/\Psi\, X$ as a function of energy at $Q^2=0$, 5, 20, and 100 GeV^2 for beryllium, iron, and lead. The solid curves and dashed curves for lead correspond to calculations with and without gluon shadowing, respectively.

The results for incoherent production of J/Ψ at $\nu_{min}=24.3$, 121.7, and 487 GeV ($l_c=1$,5 and 20 fm) are presented in Fig. 4 for beryllium, iron, and lead. We use the nonperturbative LC wave function of the photon with the parameters of the LC potential $a_{0,1}$ fixed in accordance with Eq. (30) at $v=1/2$. We use quark mass $m_c=1.5$ GeV.

Although the predicted variation of nuclear transparency with Q^2 at fixed l_c is less than for light vector meson production [10], it is still sufficiently significant to be investigated experimentally even in the range of $Q^2\lesssim 20$ GeV^2. CT effects (the rise with Q^2 of nuclear transparency) are more pronounced at low than at high energies and can be easily identified by the planned future experiments.

We also calculated the energy dependence of nuclear transparency at fixed Q^2. The results for beryllium, iron, and lead are shown in Fig. 5 for different values of Q^2. The interesting feature is the presence of a maximum of transparency at some energy, which is much more evident than in production of light vector mesons [10]. At small and moderate energies a strong rise of Tr_A^{inc} with energy, especially for the lead target, is a manifestation of net CT effects resulting from a strong inequality $l_c<l_f$. The existence of maxima of Tr_A^{inc} results from the interplay of coherence and formation effects. Indeed, the formation length rises with energy leading to an increasing nuclear transparency. At some energy, however, the effect of CL is switched on leading to a growth of the path length of the $\bar{q}q$ in the nucleus, i.e., to a suppression of nuclear transparency. This also explains the unusual ordering of curves at small and moderate Q^2 calculated for different values of l_c as is depicted in Fig. 4.

V. COHERENT PRODUCTION OF J/Ψ

First of all we present a short introduction to coherent production of vector mesons. One should replace $V\to J/\Psi$ and $\bar{q}q\to\bar{c}c$ when coherent production of charmonia is

treated. In general, in coherent (elastic) electroproduction of a vector meson the target nucleus remains intact, so all the vector mesons produced at different longitudinal coordinates and impact parameters add up coherently. This condition considerably simplifies the expressions for the production cross sections. The integrated cross section has the form

$$\sigma_A^{coh} \equiv \sigma_{\gamma^* A\to VA}^{coh} = \int d^2q \left| \int d^2b\, e^{i\vec{q}\cdot\vec{b}} \mathcal{M}_{\gamma^* A\to VA}^{coh}(b) \right|^2 = \int d^2b |\mathcal{M}_{\gamma^* A\to VA}^{coh}(b)|^2, \tag{56}$$

where

$$\mathcal{M}_{\gamma^* A\to VA}^{coh}(b) = \int_{-\infty}^{\infty} dz\, \rho_A(b,z) F_1(b,z), \tag{57}$$

with the function $F_1(b,z)$ defined in Eq. (50).

One should not use Eq. (42) for nuclear transparency anymore since the t-slopes of the differential cross sections for nucleon and nuclear targets are different and do not cancel in the ratio. Therefore, the nuclear transparency also includes the slope parameter B_V for the process $\gamma^* N\to VN$,

$$\mathrm{Tr}_A^{coh} = \frac{\sigma_A^{coh}}{A\sigma_N} = \frac{16\pi B_V \sigma_A^{coh}}{A|\mathcal{M}_{\gamma^* N\to VN}(s,Q^2)|^2}. \tag{58}$$

The energy dependent factor $C(s)$ in dipole cross section approximation Eq. (44) is adjusted in an analogical way as for incoherent charmonium production described in the preceding section. However, in contrast to Eq. (46) the factor $C(s)$ is fixed now by the following relation:

$$\frac{\int d^2b \left| \int d^2r \int d\alpha \Psi_V^{*T,L}(\vec{r},\alpha) \Psi_{qq}^{T,L}(\vec{r},\alpha) \left\{ 1-\exp\left[-\frac{1}{2} C(s) r^2 T_A(b) \right] \right\} \right|^2}{\left| \int d^2r \int d\alpha \Psi_V^{*T,L}(\vec{r},\alpha) C(s) r^2 \Psi_{qq}^{T,L}(\vec{r},\alpha) \right|^2} = \frac{\int d^2b \left| \int d^2r \int d\alpha \Psi_V^{*T,L}(\vec{r},\alpha) \Psi_{qq}^{T,L}(\vec{r},\alpha) \left\{ 1-\exp\left[-\frac{1}{2} \sigma_{qq}^-(r,s) T_A(b) \right] \right\} \right|^2}{\left| \int d^2r \int d\alpha \Psi_V^{*T,L}(\vec{r},\alpha) \sigma_{qq}^-(r,s) \Psi_{qq}^{T,L}(\vec{r},\alpha) \right|^2}. \tag{59}$$

A. Predictions for coherent production of J/Ψ

Unfortunately, there are no data yet on coherent electroproduction of charmonia. Therefore, we present only predictions that can be later verified and tested in the future planned experiments.

One can eliminate the effects of CL and single out the net CT effect in a way similar to what was suggested for incoherent reactions by selecting experimental events with l_c = const. We calculated nuclear transparency for the coherent reaction $\gamma^* A\to J/\Psi A$ at fixed values of l_c. The results for $l_c = 1$, 5, and 20 fm are depicted in Fig. 6 for several nuclei. We performed calculations of Tr_A^{coh} with the slope $B_V = B_{J/\Psi} = 4.7\ \mathrm{GeV}^{-2}$. The effect of a rise of Tr_A^{coh} is not sufficiently large to be observable in the range of $Q^2 \leqslant 20\ \mathrm{GeV}^2$. A wider range of $Q^2 \leqslant 100\ \mathrm{GeV}^2$ and heavy nuclei gives higher chances for experimental investigation of CT. However, it encounters the problem of low yields at high Q^2.

Note that in contrast to incoherent production where nuclear transparency is expected to saturate as $\mathrm{Tr}_A^{inc}(Q^2) \to 1$ at large Q^2, for the coherent process nuclear transparency reaches a higher limit, $\mathrm{Tr}_A^{coh}(Q^2) \to A^{1/3}$.

We also calculated nuclear transparency as function of energy at fixed Q^2. The results for J/Ψ produced coherently off beryllium, iron, and lead are depicted in Fig. 7 at Q^2 = 0, 5, 20, and 100 GeV^2. Tr_A^{coh} is very small at low energy, which of course does not mean that nuclear matter is not transparent, but the nuclear coherent cross section is suppressed by the nuclear form factor. Indeed, the longitudinal momentum transfer which is equal to the inverse CL, is large when the CL is short. However, at high energy $l_c \gg R_A$ and nuclear transparency nearly saturates (it decreases with ν only due to the rising dipole cross section). The saturation level is higher at larger Q^2, which is a manifestation of CT.

Note that in all calculations the effects of gluon shadowing are included in a way analogical to that described in the recent papers [10,11]. They are much smaller than in production of light vector mesons. For illustration, they are depicted in Figs. 5 and 7 for the lead target as a difference between solid and dashed lines at various values of Q^2. In the photoproduction limit $Q^2 = 0$ the onset of gluon shadowing becomes important at rather high photon energy $\nu > 1000$ GeV for incoherent and $\nu > 500$ GeV for coherent production. This corresponds to the claim made in Ref. [15] that the onset of gluon shadowing requires smaller x_{Bj} than the onset of quark shadowing. The reason is that the fluctuations containing gluons are, in general, heavier than the $\overline{q}q$ and have a shorter CL.

Although gluon shadowing is included in all calculations, it is small enough in the kinematic range important for in-

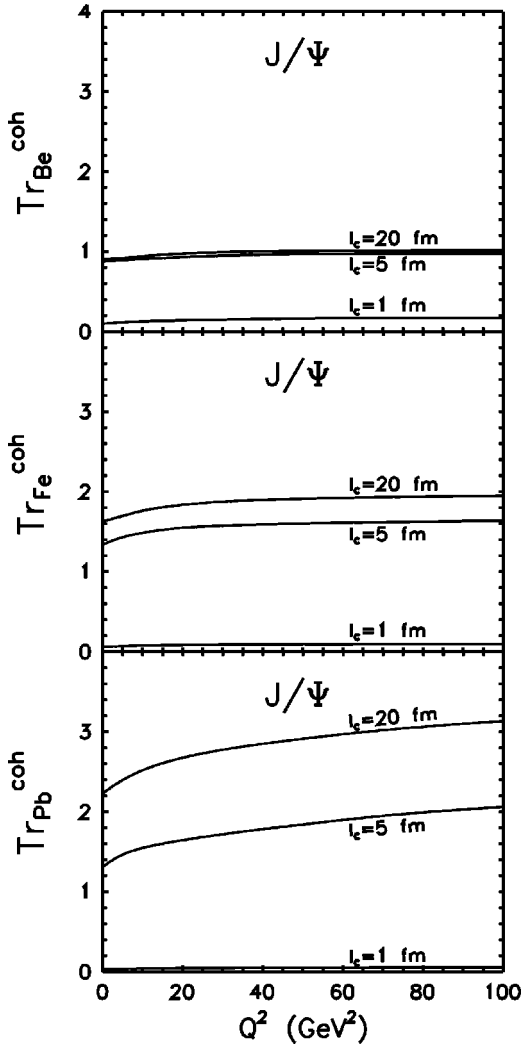

FIG. 6. The same as in Fig. 4, but for coherent production of J/Ψ, $\gamma^* A \to J/\Psi\, A$.

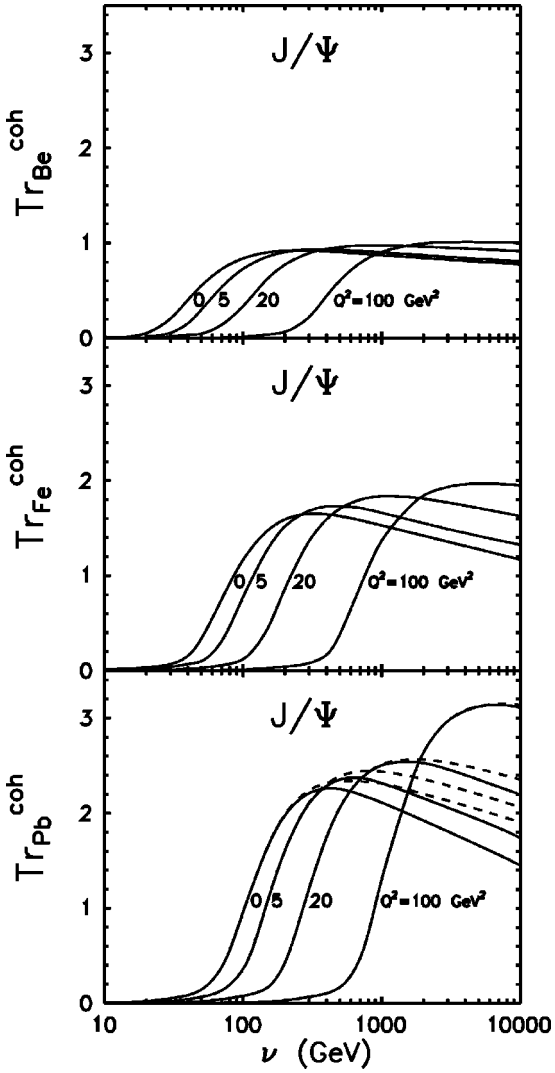

FIG. 7. Nuclear transparency for coherent electroproduction $\gamma^* A \to J/\Psi\, A$ as a function of energy at $Q^2 = 0$, 5, 20, and 100 GeV^2 for beryllium, iron, and lead. The solid curves and dashed curves for lead correspond to calculations with and without gluon shadowing, respectively.

vestigation of CT. Consequently, it does not affect the main achievements and conclusions important in the process of searching for CT effects in charmonium coherent and incoherent production off nuclei.

VI. SUMMARY AND CONCLUSIONS

In the present paper we focused the main emphasis on the production of charmonia due to advantages as compared with light vector meson production [10]. Electroproduction of charmonia off nuclei is a very convenient way to study the interplay between coherence (shadowing) and formation (color transparency) effects. A strong inequality $l_c < l_f$ in all kinematic region of ν and Q^2 leads to a different scenario of mixing of CT and CL effects as compared to light vector mesons where $l_c \gtrsim l_f$ at $Q^2 \lesssim 1-2$ GeV^2. Consequently, at small and moderate energies a problem of CT-CL separation is not so acute. Besides, due to quite a large mass of the c quark the relativistic corrections and nonperturbative effects are sufficiently small. They are negligible investigating the production of still heavier vector mesons (bottonium, toponium). However, one encounters the problem of very low yields as well as very small CT and CL effects (due to very large masses of $\bar{q}q$ fluctuactions and vector mesons) to be measured experimentally. Therefore production of charmonia represents some compromise, because the above mentioned theoretical uncertainties (typical for light vector mesons) and very small production rates (typical for still heavier vector mesons) are eliminated to a certain extent keeping sufficiently large CT and CL effects. This fact supports an enhanced interest to study electroproduction of charmonia off nuclei separately. We used from Ref. [10] a rigorous quantum-mechanical approach based on the light-cone QCD Green function formalism which naturally incorporates the interference effects of CT and CL. Our main results and observations are the following.

Within the suggested approach taken from Ref. [10], interpolating between the previously known low- and high-energy limits we studied for the first time CT effects in co-

herent and incoherent electroproduction of charmonia off nuclei.

As the first test we compare the model predictions with available data from the NMC experiment on energy dependence of the nuclear transparency ratio $\mathrm{Tr}_{Sn}^{inc}/\mathrm{Tr}_{C}^{inc}$ for incoherent production of J/Ψ at $Q^2=0$. We found a good agreement with the data, which confirms the dominance of CT effects at small and medium and CL effects at medium large and large energies.

The onset of coherence effects (shadowing) can mimic the expected signal of CT in incoherent electroproduction of charmonia at medium large and large energies. In order to single out the formation effect the data must be taken at such energy and Q^2 which keep $l_c=\mathrm{const}$. Then the observation of a rise with Q^2 of nuclear transparency for fixed l_c would give a signal of color transparency. Predictions of $\mathrm{Tr}_{A}^{inc}(Q^2)$ as a function of Q^2 at different fixed l_c show rather large CT effects in incoherent production of charmonia. Although the variation of nuclear transparency with Q^2 at fixed l_c is predicted to be less than for the production of light vector mesons [10], it is still sufficiently significant to be investigated experimentally even in the range of $Q^2 \lesssim 20\ \mathrm{GeV}^2$. CT effects (the rise with Q^2 of nuclear transparency) are more pronounced at low than at high energies and can be easily identified by the planned future experiments.

The effects of CT in coherent production of charmonia are found to be less pronounced, similarly as in production of light vector mesons [10]. A wider range $Q^2 \leqslant 100\ \mathrm{GeV}^2$ and heavy nuclei give higher chances for experimental investigation of CT. However, it faces the problem of low yields at high Q^2.

The effects of gluon shadowing were shown to be important only at much higher energies than in production of light vector mesons due to large mass of $\bar{c}c$ fluctuation. Nuclear suppression of gluons was calculated within the same LC approach and included in predictions. It was manifested that these corrections are quite small at medium energies which are dominant in the process of searching for CT effects.

Finally, one can compare the predictions for incoherent and coherent charmonium production off lead target (see Figs. 4, 5, 6, and 7) obtained within rigorous quantum-mechanical approach based on the light-cone QCD Green function formalism (incorporating naturally CT and CL effects) with the results of Ref. [11] evaluated in the approximation of long coherence length $l_c \gg R_A$ (without CT effects) allow to employ realistic light-cone wave functions of charmonia from Ref. [13] and to make corrections for finite values of l_c. We find a nice quantitative agreement at moderate and high energies and at low and medium values of Q^2. This fact confirms justification to use that high-energy approximation [11] for charmonium electroproduction off nuclei in the kinematic region where CL effects dominate. Besides, using advantages from both approaches, one can perform in the future fully realistic calculations using known LC dipole approach based on Green function formalism employing a realistic dipole cross section and using realistic LC wave functions of charmonia from [13].

In conclusion, the predicted rather large effects of CT in incoherent electroproduction of charmonia off nuclei open further possibilities to search for CT with medium energy electrons and can be tested in future experiments.

ACKNOWLEDGMENTS

This work was supported in part by the Slovak Funding Agency, Grant Nos. 2/1169 and 6114.

[1] T. Matsui and H. Satz, Phys. Lett. B **178**, 416 (1986).
[2] V.N. Gribov, Zh. Éksp. Teor. Fiz. **56**, 892 (1969) [Sov. Phys. JETP **29**, 483 (1969)].
[3] A.B. Zamolodchikov, B.Z. Kopeliovich, and L.I. Lapidus, Pis'ma Zh. Tekh. Fiz. **33**, 612 (1981) [JETP Lett. **33**, 595 (1981)].
[4] G. Bertsch, S.J. Brodsky, A.S. Goldhaber, and J.F. Gunion, Phys. Rev. Lett. **47**, 297 (1981).
[5] J.F. Gunion and D.E. Soper, Phys. Rev. D **15**, 2617 (1977).
[6] J. Hüfner and B. Povh, Phys. Rev. D **46**, 990 (1992).
[7] B. Povh, hep-ph/9806379.
[8] B.Z. Kopeliovich and B.G. Zakharov, Phys. Rev. D **44**, 3466 (1991).
[9] J. Hüfner and B.Z. Kopeliovich, Phys. Lett. B **403**, 128 (1997).
[10] B.Z. Kopeliovich, J. Nemchik, A. Schaefer, and A.V. Tarasov, Phys. Rev. C **65**, 035201 (2002).
[11] Yu.P. Ivanov, B.Z. Kopeliovich, A.V. Tarasov, and J. Huefner, Phys. Rev. C **66**, 024903 (2002).
[12] J. Hüfner, B.Z. Kopeliovich, and J. Nemchik, Phys. Lett. B **383**, 362 (1996).
[13] J. Huefner, Yu.P. Ivanov, B.Z. Kopeliovich, and A.V. Tarasov, Phys. Rev. D **62**, 094022 (2000).
[14] K. Golec-Biernat and M. Wüsthoff, Phys. Rev. D **59**, 014017 (1999); **60**, 114023 (1999).
[15] B.Z. Kopeliovich, A. Schäfer, and A.V. Tarasov, Phys. Rev. D **62**, 054022 (2000).
[16] A. Donnachie and P.V. Landshoff, Phys. Lett. B **478**, 146 (2000).
[17] Particle Data Group, D.E. Groom *et al.*, Eur. Phys. J. C **15**, 1 (2000).
[18] J.B. Bronzan, G.L. Kane, and U.P. Sukhatme, Phys. Lett. **49B**, 272 (1974).
[19] J.B. Kogut and D.E. Soper, Phys. Rev. D **1**, 2901 (1970).
[20] J.M. Bjorken, J.B. Kogut, and D.E. Soper, Phys. Rev. D **3**, 1382 (1971).
[21] N.N. Nikolaev and B.G. Zakharov, Z. Phys. C **49**, 607 (1991).
[22] R.P. Feynman and A.R. Gibbs, *Quantum Mechanics and Path Integrals* (McGraw-Hill, New York, 1965).
[23] H1 Collaboration, S. Aid *et al.*, Z. Phys. C **69**, 27 (1995).
[24] ZEUS Collaboration, M. Derrick *et al.*, Phys. Lett. B **293**, 465 (1992).
[25] M.V. Terent'ev, Yad. Fiz. **24**, 207 (1976) [Sov. J. Nucl. Phys. **24**, 106 (1976)].
[26] J. Nemchik, N.N. Nikolaev, E. Predazzi, and B.G. Zakharov, Z. Phys. C **75**, 71 (1997).

[27] I. Halperin and A. Zhitnitsky, Phys. Rev. D **56**, 184 (1997).
[28] H1 Collaboration, C. Adloff *et al.*, Phys. Lett. B **483**, 23 (2000).
[29] H1 Collaboration, C. Adloff *et al.*, Eur. Phys. J. C **10**, 373 (1999).
[30] ZEUS Collaboration, J. Breitweg *et al.*, Eur. Phys. J. C **6**, 603 (1999).
[31] E401 Collaboration, M. Binkley *et al.*, Phys. Rev. Lett. **48**, 73 (1982).
[32] E516 Collaboration, B.H. Denby *et al.*, Phys. Rev. Lett. **52**, 795 (1984).
[33] ZEUS Collaboration, J. Breitweg *et al.*, Z. Phys. C **75**, 215 (1997).
[34] B.Z. Kopeliovich, J. Raufeisen, and A.V. Tarasov, Phys. Lett. B **440**, 151 (1998).
[35] B.Z. Kopeliovich, J. Raufeisen, and A.V. Tarasov, Phys. Rev. C **62**, 035204 (2000).
[36] J. Hüfner, B.Z. Kopeliovich, and A. Zamolodchikov, Z. Phys. A **357**, 113 (1997).
[37] B.Z. Kopeliovich, J. Nemchik, N.N. Nikolaev, and B.G. Zakharov, Phys. Lett. B **324**, 469 (1994).
[38] E665 Collaboration, M.R. Adams *et al.*, Phys. Rev. Lett. **74**, 1525 (1995).
[39] B.Z. Kopeliovich and J. Nemchik, nucl-th/9511018.
[40] NMC Collaboration, M. Arneodo *et al.*, Phys. Lett. B **332**, 195 (1994).